Supporting Information

Tumor-penetrating Peptide Conjugated and Doxorubicin Loaded T_1-T_2 Dual Mode MRI Contrast Agents Nanoparticles for Tumor Theranostics

Lipeng Gao[1], Jing Yu[1], Yang Liu[1], Jinge Zhou[1], Lei Sun[1], Jing Wang[1], Jianzhong Zhu[1], Hui Peng[2], Weiyue Lu[3], Lei Yu[1], Zhiqiang Yan[1]✉, Yiting Wang[1]✉

1. Institute of Biomedical Engineering and Technology, Shanghai Engineering Research Center of Molecular Therapeutics and New Drug Development, School of Chemistry and Molecular Engineering, East China Normal University, Shanghai 200062, China.
2. Key Laboratory of Polar Materials and Devices, Ministry of Education, School of Information Science and Technology, East China Normal University, Shanghai 200241, China.
3. Department of Pharmaceutics, School of Pharmacy, Fudan University & Key Laboratory of Smart Drug Delivery, Fudan University, Ministry of Education, Shanghai 201203, China.

✉ Corresponding authors: zqyan@sat.ecnu.edu.cn, ytwang@nbic.ecnu.edu.cn

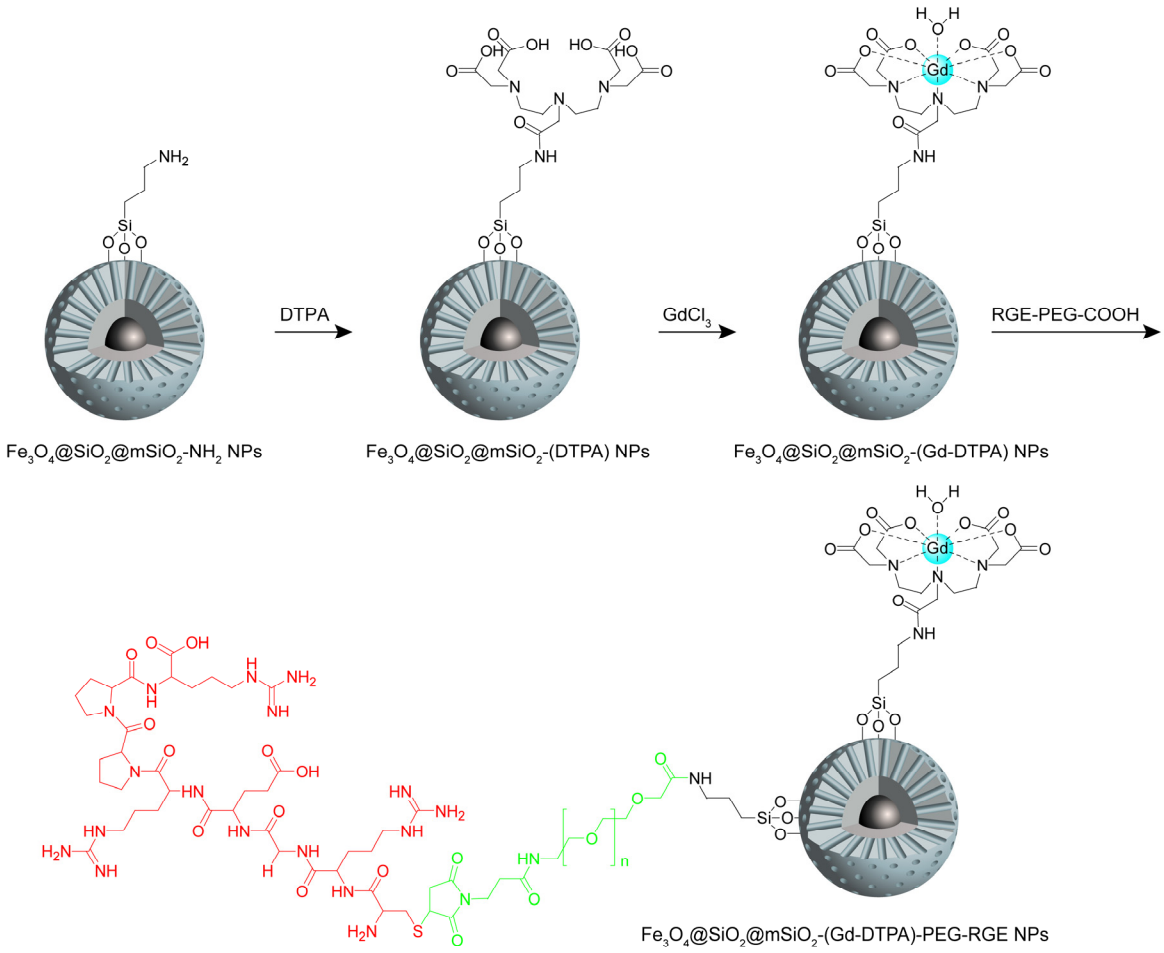

Figure S1 The synthetic scheme of Fe_3O_4@SiO_2@mSiO_2-(Gd-DTPA)-PEG-RGE NPs. The red part is RGERPPR peptide, and the green is PEG chain.

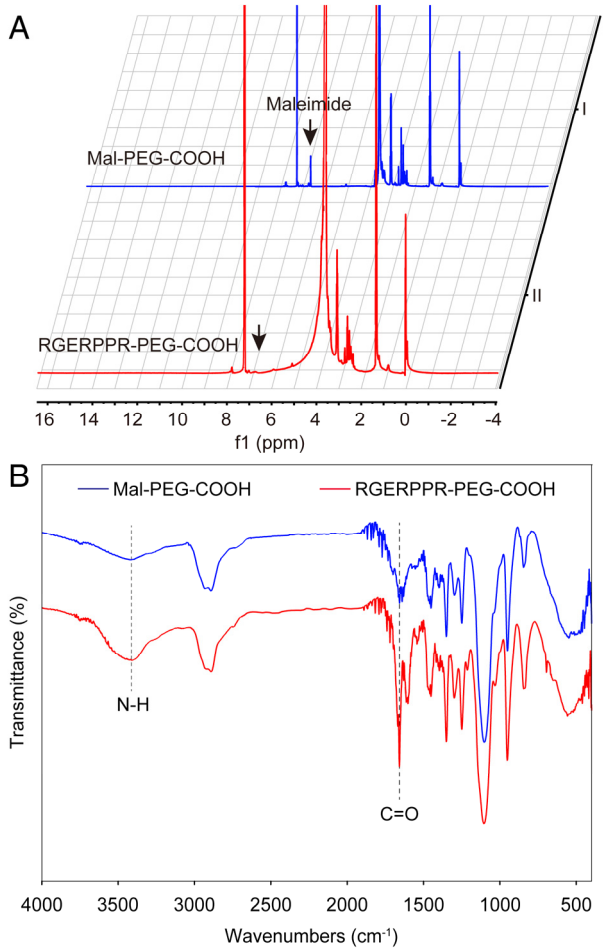

Figure S2. The ^{1}H-NMR spectra (A) and FTIR spectra (B) of Mal-PEG-COOH and RGERPPR-PEG-COOH. The characteristic peak of maleimide group at 6.7 ppm can be found in ^{1}H-NMR spectrum of Mal-PEG-COOH, but disappears in that of RGERPPR-PEG-COOH; the intensity of both N-H at 3200-3600 cm^{-1} and C=O band at 1658 cm^{-1} significantly enhanced in the FTIR spectrum of RGERPPR-PEG-COOH compared with that of Mal-PEG-COOH.

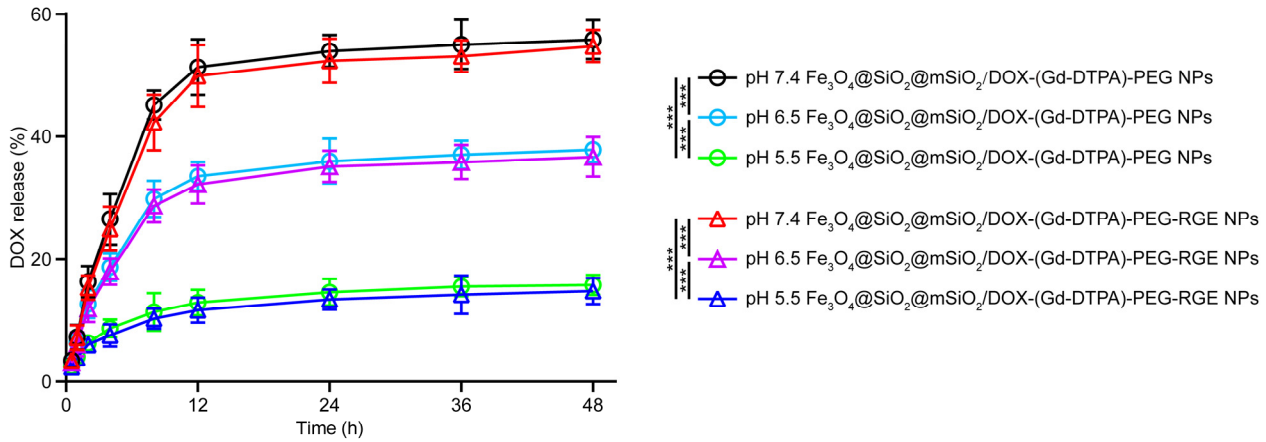

Figure S3. DOX release profiles from NPs at pH 5.5, pH 6.5 and pH 7.4. DOX release from the two types of NPs was remarkably increased as the pH decreased.

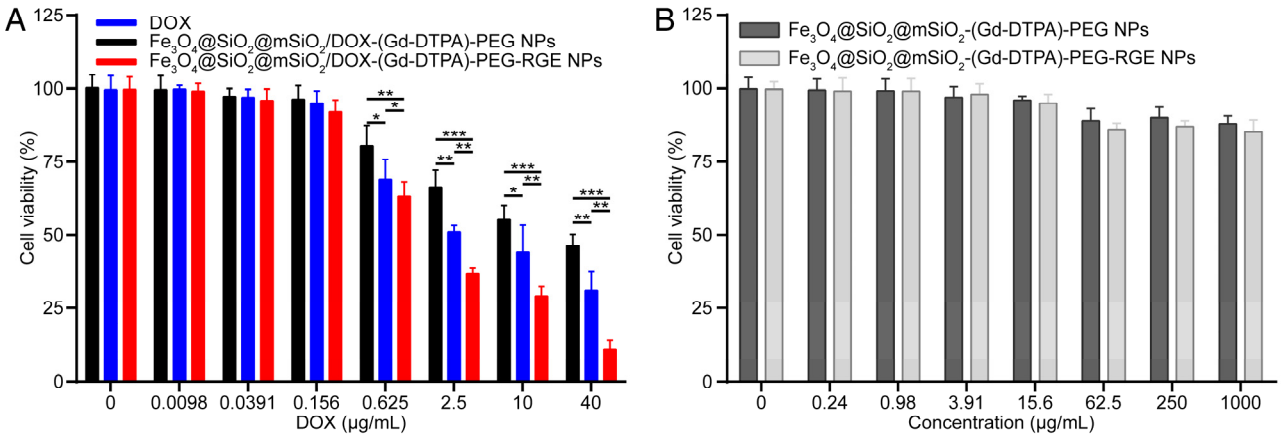

Figure S4. The in vitro cytotoxicity of Fe_3O_4@SiO_2@mSiO_2/DOX-(Gd-DTPA)-PEG-RGE NPs (A) and those without DOX loading (B).

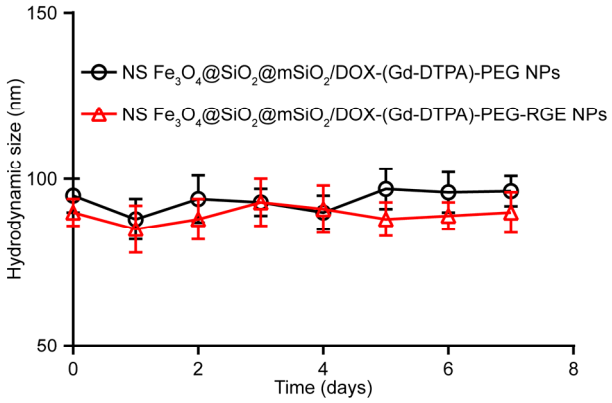

Figure S5. The stability of NPs in normal saline (NS) solution.

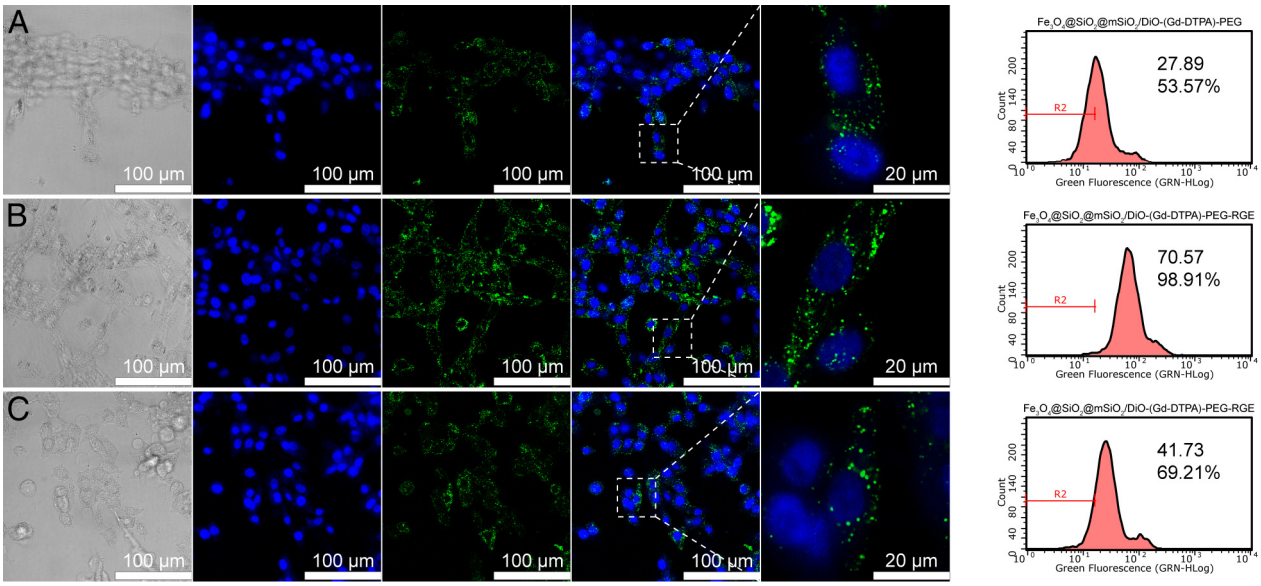

Figure S6. The CLSM images of cellular uptake and flow cytometry for Fe_3O_4@SiO_2@mSiO_2/DiO-(Gd-DTPA)-PEG NPs (A), Fe_3O_4@SiO_2@mSiO_2/DiO-(Gd-DTPA)-PEG-RGE NPs (B) and EG00229 pre-treatment plus Fe_3O_4@SiO_2@mSiO_2/DiO-(Gd-DTPA)-PEG-RGE NPs (C). The numbers in flow cytometry images represent mean of fluorescence intensity and percentages of DiO-positive cells, respectively. The cellular uptake of Fe_3O_4@SiO_2@mSiO_2/DiO-(Gd-DTPA)-PEG-RGE NPs by U87MG cells was significant increased compared with the other two groups.

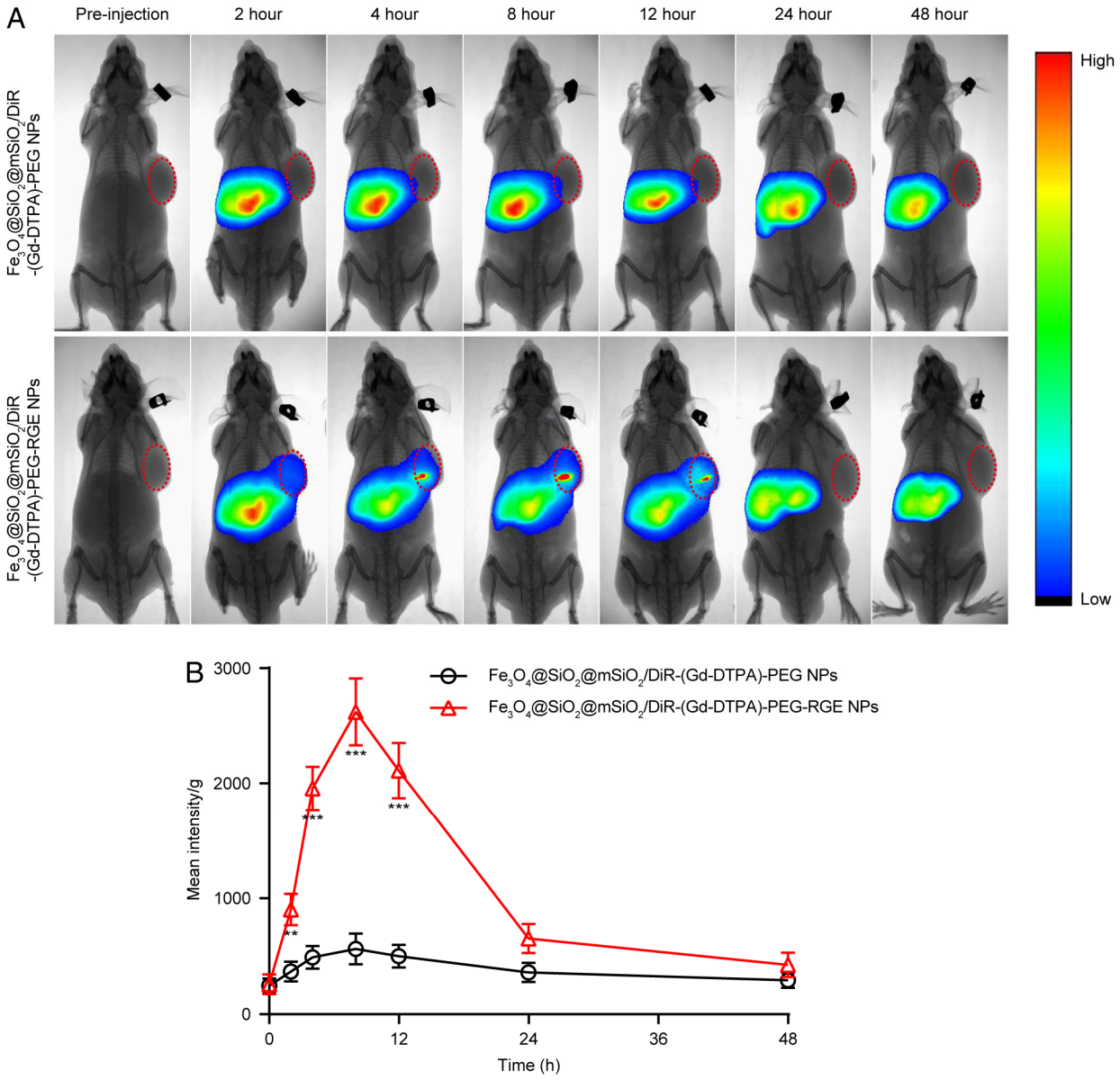

Figure S7. In vivo fluorescent imaging of Fe_3O_4@SiO_2@mSiO_2/DiR-(Gd-DTPA)-PEG NPs and Fe_3O_4@SiO_2@mSiO_2/DiR-(Gd-DTPA)-PEG-RGE NPs. (A) Representative in vivo fluorescent images of U87MG tumor-bearing mice (n = 3) following i.v. administration of NPs at different time points. Color bar on the right side indicates the signal intensity of the fluorescence. (B) The pharmacokinetic profile of DiR in tumor tissue based on the semi-quantitative ROI analysis of in vivo fluorescent images.

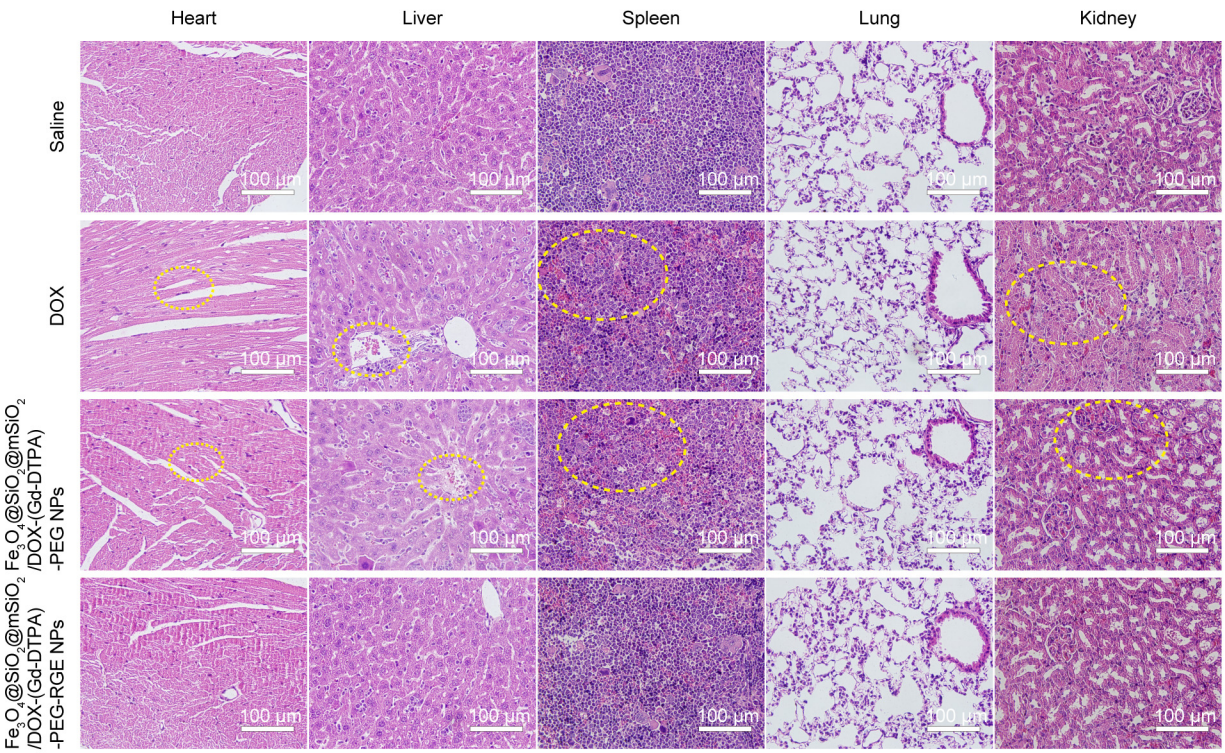

Figure S8. The H&E staining slides of the main organs of U87MG tumor-bearing mice (n = 3) after the treatment with Saline (control), DOX, Fe_3O_4@SiO_2@mSiO_2/DOX-(Gd-DTPA)-PEG NPs, and Fe_3O_4@SiO_2@mSiO_2/DOX-(Gd-DTPA)-PEG-RGE NPs (40×). The main organs (including heart, liver, spleen, lung, and kidney) of the Fe_3O_4@SiO_2@mSiO_2/DOX-(Gd-DTPA)-PEG-RGE NPs group showed no obvious pathological abnormity compared with Saline groups.

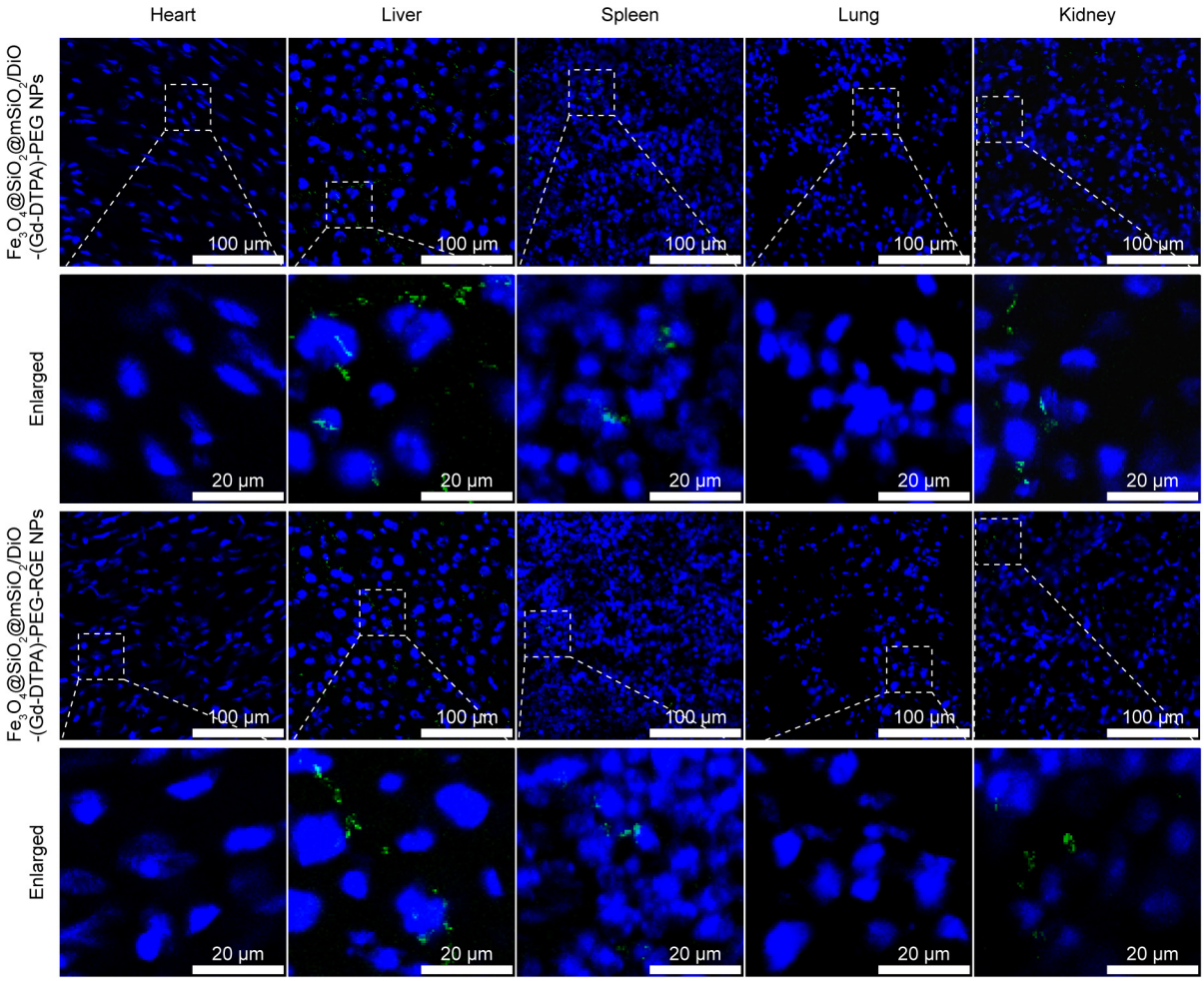

Figure S9. The CLSM images of frozen the main organs of U87MG tumor-bearing mice (n = 3) following injection of Fe_3O_4@SiO_2@mSiO_2/DiO-(Gd-DTPA)-PEG NPs and Fe_3O_4@SiO_2@mSiO_2/DiO-(Gd-DTPA)-PEG-RGE NPs.